Separation Science and Technology
Publication details, including instructions for authors and subscription information:
http://www.informaworld.com/smpp/title~content=t713708471

TAYLOR VORTEX COLUMN: LARGE SHEAR FOR LIQUID-LIQUID EXTRACTION

L. J. Forney[a]; A. H. P. Skelland[a]; J. F. Morris[a]; R. A. Holl[b]
[a] School of Chemical Engineering, Georgia Tech, Atlanta, GA, U.S.A. [b] Holl Technologies Co., Camarillo, CA, U.S.A.

Online publication date: 09 September 2002

To cite this Article Forney, L. J. , Skelland, A. H. P. , Morris, J. F. and Holl, R. A.(2002) 'TAYLOR VORTEX COLUMN: LARGE SHEAR FOR LIQUID-LIQUID EXTRACTION', Separation Science and Technology, 37: 13, 2967 — 2986
To link to this Article: DOI: 10.1081/SS-120005644
URL: http://dx.doi.org/10.1081/SS-120005644

MARCEL DEKKER, INC. • 270 MADISON AVENUE • NEW YORK, NY 10016

SEPARATION SCIENCE AND TECHNOLOGY, 37(13), 2967–2986 (2002)

TAYLOR VORTEX COLUMN: LARGE SHEAR FOR LIQUID–LIQUID EXTRACTION

L. J. Forney,[1,*] A. H. P. Skelland,[1] J. F. Morris,[1] and R. A. Holl[2]

[1]School of Chemical Engineering, Georgia Tech, Atlanta, GA 30332
[2]Holl Technologies Co., Camarillo, CA 93012

ABSTRACT

A Taylor vortex column provides a large shear in the absence of form drag in contrast to other common mixing devices. In particular, the power per unit mass for a column is expressed in terms of a torque coefficient and compared with similar expressions for both, a stirred tank (power number) and a static mixer (friction factor). Results of computational fluid dynamic computations provide a picture of essential features of the flowfield. Moreover, experiments with a prototype Taylor column are presented for the continuous liquid–liquid extraction of benzoic acid from toluene to water. Arguments are presented for the observed increase in stage efficiency with larger volume fractions of dispersed toluene.

Key Words: Liquid–liquid extraction; Taylor vortex

*Corresponding author. Fax: (404) 894-4200; E-mail: larry.forney@che.gatech.edu

INTRODUCTION

Common mixing devices such as stirred tanks or static mixers pose potential problems in shear-sensitive mixing applications as listed in Table 1. Examples of the latter are biological solids in fermentation processes or emulsions where particle integrity and coagulation are affected. In particular, the scale-up of stirred tanks with constant power/volume will increase the maximum shear rate, which can represent a serious limitation.[1,2] Problems also exist with static mixers since the maximum shear is inversely proportional to the fluid residence time.

Moreover, much of the energy consumed in either stirred tanks or static mixers is due to the action of form drag on blunt impeller blades or static mixer elements. In contrast, a Taylor vortex column shown in Fig. 1 consumes much of the power through friction drag and is also relatively simple to scale-up. In fact, one can easily scale-up a Taylor column with equal power/volume, as well as shear stress.

Taylor vortex flow is the result of an unstable pressure gradient on a fluid between coaxial cylinders. Many mass transfer studies have been performed with the common configuration of a single fluid between rotating inner and stationary outer cylinders as summarized by Baier et al.[3] In contrast, little work has been performed with two immiscible liquid phases. Examples of the latter are extraction in dispersed two-fluid flow.[4–6] Recent studies have also been performed to characterize mass transfer in radially stratified two-fluid flows that are useful if one wishes to eliminate emulsification.[7,8]

In the present study, computational fluid dynamic (CFD) computations are performed with a single fluid to characterize fluid properties such as eddy dispersion, effective viscosity, and shear stress. Moreover, the extraction efficiency of benzoic acid from toluene to water was measured in a prototype Taylor column. These continuous flow, single-stage efficiency data were measured vs. power input and the results were compared with published extraction stage efficiency of a substantially larger stirred tank.

Table 1. Shear-Sensitive Mixing

Two phases	Gas–liquid
	Liquid–liquid
	Solid–liquid
Applications	Fermentation
	Waste treatment
	Emulsions
	Extraction
	Polymerization
	Crystallization
	Flocculation

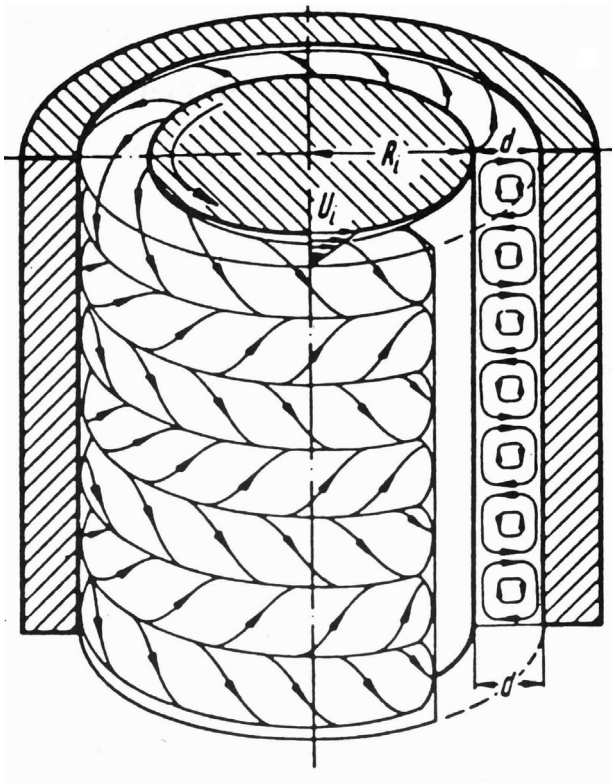

Figure 1. Taylor vortices between two concentric cylinders. Inner cylinder rotating, outer cylinder at rest; d is the width of annular gap; h the height of cylinder.[9]

SCALE-UP

The torque coefficient C_m for the Taylor column is independent of the device geometry. This is in contrast to the analogous dimensionless groups of friction factor f for a static mixer or power number N_p for a stirred tank. For example, the friction factor depends on geometry (void space and mixing element design) in a static mixer while the power number in a stirred tank depends on both the number of impellers and baffles and their geometry.

Thus, scale-up in turbulent flow is much simpler for the Taylor column and is limited to one dimensionless group called the Taylor number[9] defined as

$$Ta = \frac{U_i d}{\nu}\sqrt{\frac{d}{R_i}} \tag{1}$$

where d is the gap width, R_i the radius of the rotating column, $U_i(= \omega R_i)$ is the peripheral velocity of the rotating column, and ν is the kinematic viscosity as shown in Fig. 1. Likewise, the important group for laminar flow ($Ta < 400$) is the Reynolds number dU_i/ν.

In addition, since both the power/volume and shear stress in a Taylor column depends on the gap width d and peripheral velocity U_i, one can independently increase the fluid volume of the device $\sim 2\pi R_i(dh)$ by simply increasing the radius of the rotating column R_i and column length h. For turbulent flow ($Ta > 400$), such an increase in size will have a minor effect on both the torque coefficient C_m and power/volume since $C_m \propto (Ta)^{-1/5}$ and $Ta \propto (R_i)^{-1/2}$.

POWER CONSUMPTION

Mixers impart energy to fluids. The power input to a fluid is the result of the action of either friction or form drag by the fluid on the solid surfaces of the mixer as shown in Fig. 2. The nature of the surface would depend on the mixer design. For example, form drag on the impellers in a stirred tank or mixing elements in a static mixer is responsible for power consumption.

Clearly, friction drag is the dominant mechanism for power consumption in a Taylor column. The characteristics of a stirred tank, static mixer, and Taylor column are listed in Table 2. Expressions for power consumption are listed in Table 3 along

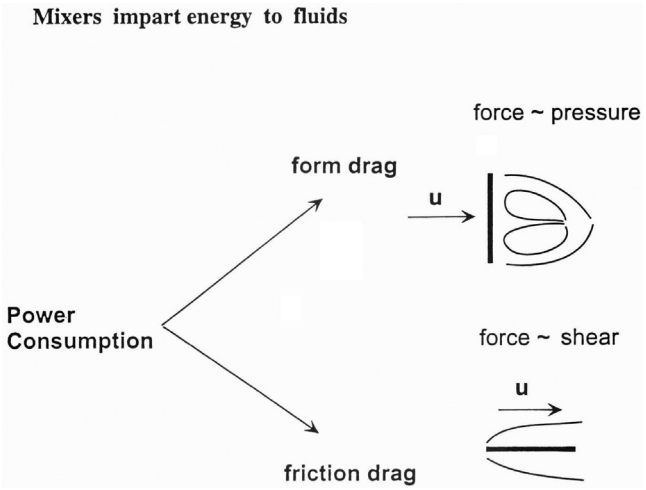

Figure 2. Power consumption.

Table 2. Characteristics of Mixing Devices

Design	Characteristics
Stirred tank	Form drag Nonuniform shear
Static mixer	Form drag Shear/resident time
Taylor column	Friction drag Power efficient

with the appropriate dimensionless groups. In all cases the power/mass is proportional to the cube of the characteristic velocity divided by a length.

Table 4 provides order of magnitude estimates for the total power/mass for each mixing device. These calculations are based on a fluid volume of 500 cm^3 along with a characteristic velocity $u = 1\,m/sec$ and a length of 1 cm. The velocity

Table 3. Expressions for Power Consumption

Design	Power/Mass	Group
Stirred tank	$\dfrac{N_p}{\left(\frac{27}{4}\right)\pi^4}\left[\dfrac{u^3}{D}\right]$	N_p = power number
Static mixer	$2\dfrac{f}{\alpha}\left[\dfrac{u^3}{D}\right]$	f = friction factor
Taylor column	$\dfrac{C_m}{4}\left[\dfrac{u^3}{d}\right]$	C_m = torque coefficient

Table 4. Power Consumption

Design[a]	Total Power/Mass (watts/kg)	Friction Drag Power/Mass (watts/kg)
Stirred tank	$\sim 10^{-1}$–1	$\sim 10^{-2}$
Static mixer	$\sim 10^{2}$	$\sim 10^{-1}$
Taylor column	$\sim 10^{-1}$	$\sim 10^{-1}$

[a] $u = 1\,m/sec$, length = 1 cm, volume ~ 500 mL, maximum shear = $(1\,m/sec)/(0.01\,m) = 10^2(sec^{-1})$. Length is either: width of the impeller (stirred tank), diameter of the mixing element (static mixer), or gap width (Taylor column). Stirred tank: diameter = 9 cm, height = 9 cm. Static mixer: pipe diameter = 5 cm, length = 25 cm. Taylor column: radius = 5 cm, length = 15 cm.

corresponds to the tip speed of the impeller for the stirred tank, superficial fluid velocity in the static mixer, or surface (tangential) velocity of the rotating column in the Taylor device. The length, moreover, is either the width of the impeller blade, diameter of a mixing element, or the gap width in the Taylor column.

Hence, for all three devices in Table 4 the typical shear is the ratio of velocity-to-length or a constant $10^2\ \text{sec}^{-1}$. The product of the fluid velocity, area of the moving surface, fluid viscosity, and shear rate now gives an order of magnitude estimate of power/mass consumed as friction drag, which is also listed. These results would suggest that shear-sensitive mixing favors the Taylor column at lower energy costs.

RESIDENCE TIME

Recent measurements of the cumulative residence time distribution (RTD) are shown in Fig. 3 for the Taylor column.[10] Small Taylor numbers are equivalent to a large number of stirred tanks in series while large values of *Ta* are related to a small number of tanks approaching one as discussed by Moore and

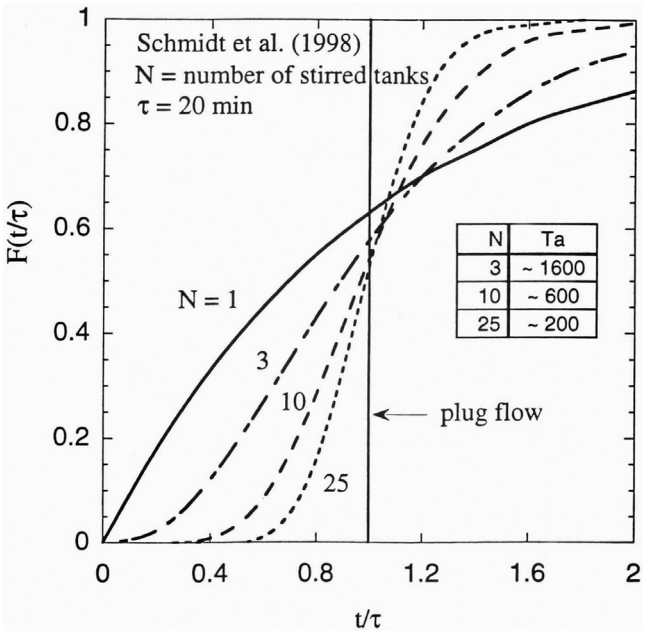

Figure 3. Effect of Taylor number on cumulative RTD.

Cooney.[11] The fluid resident time was found to have a much smaller effect than the Taylor number on the number of equivalent tanks in series. These results would suggest that a single Taylor column could be used for applications requiring either plug flow or continuous stirred tank reactor (CSTR) characteristics by simply increasing the rpm.

COMPUTATIONAL FLUID DYNAMIC SIMULATIONS

The fluid dynamic behavior of the Taylor column has been characterized with a commercial CFD code (Fluent version 4.48). Figure 4 shows the stream function for a value of the turbulent Taylor number $Ta = 600$. The dimensions of the 2D grid are $R_i = 1$ cm, $d = 2$ mm, and a column length of $h = 2$ cm rotating such that $U_i = 10$ m/sec (into page) on the left wall. The axial dimension covering the range $0 < x < 2$ cm measured from top-to-bottom contains four counter rotating vortices with an interface between two such vortices occurring at $x = 0.5$, 0.9, and 1.38 cm. The first vortex rotates in the counter clockwise direction giving two stagnation points on the right wall at $x = 0.5$ and 1.35 cm along with one stagnation point at $x = 0.9$ cm on the left wall.

Figure 5 shows the radial velocity vs. axial distance along the center of the gap at $y = 1$ mm where y is the radial dimension across the gap such that $0 < y < 2$ mm. The peak radial velocities are shown to be less than 10% of the peripheral column velocity U_i.

Figure 6 shows the asymmetry in the turbulent dissipation rate vs. axial distance near the top stationary wall at $y = 1.93$ mm. The peaks are shown to occur at the stagnation points. Figure 7 shows the values of the eddy dissipation rate across the gap between two vortices at an axial distance of 1.38 cm with the large peak occurring near the top stagnation point.

Figures 8 and 9 represent the asymmetry in the peripheral velocity and effective viscosity across the gap at the center of a vortex ($x = 0.67$ cm) and between two vortices ($x = 1.31$cm). These two figures provide the necessary data for Fig. 10, which shows the peripheral shear stress across the gap.

LIQUID–LIQUID EXTRACTION

Geometry

The simplicity of scale-up is demonstrated with a small model of a Taylor column. The model shown in Fig. 11 has a 6-cm^3 holdup volume, a 2-cm long rotating aluminum cylinder with a gap width of $d = 2$ mm, and a radius of $R_i = 1$ cm. These are the same dimensions used in the numerical CFD simulation

Figure 4. Stream function for water in 2-mm gap at $Ta = 600$.

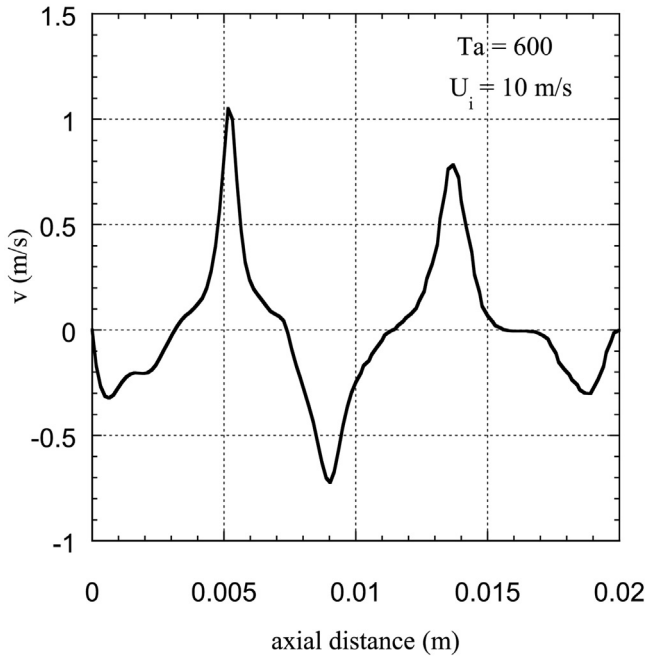

Figure 5. Radial velocity along center of gap.

in "Computational Fluid Dynamic Simulations." Moreover, the shaft and bearing assembly is similar to the design used in stirred tanks.

Experimental Procedure

A common liquid–liquid extraction of benzoic acid from toluene to water was carried out in the model Taylor column. Such a system is mass transfer limited on the water side.[12] Two sets of experiments were performed at water-to-toluene mass flow ratios of 1.2 and 11. In both cases, a mixture of 11 g of benzoic acid per 500 mL toluene (0.18 gmol/L) was combined in the Taylor column with 6 mL per min of pure water.

After an equilibrium flow was established, a 5-min sample of the output stream was collected in a Erlenmeyer flask. The lighter toluene fraction was immediately decanted from the top. The concentration of benzoic acid M_ω was determined by titration of a 20 mL pipetted sample with a 0.1 N NaOH (phenolphthalein indicator).

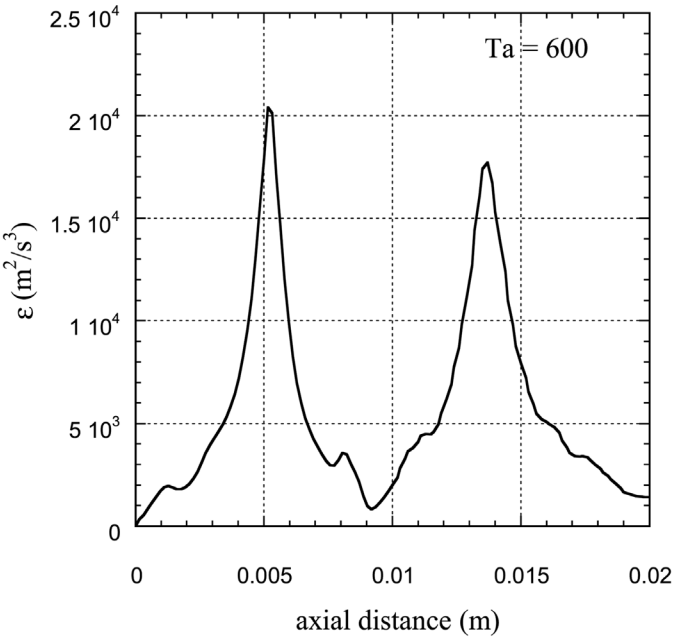

Figure 6. Eddy dissipation near stationary wall.

Similar measurements of benzoic acid concentration M_o in water were made at zero rpm for each of the two mass flow ratios along with a number of data points of concentration M_ω with increasing rpm. Moreover, the equilibrium benzoic acid concentration M_e was established for each mass flow ratio by combining a volume ratio of either 1:1 or 9.5:1 for the water and the toluene/benzoic acid mixture and stirring for a period of 30 min.

The single-stage efficiency E_a attributable to agitation was computed in the form suggested by Flynn and Treybal[13]

$$E_a = \frac{M_\omega - M_o}{M_e - M_o} \tag{2}$$

or

$$E_a = \frac{E - E_o}{1 - E_o} \tag{3}$$

where $E_o = M_o/M_e$ is the stage efficiency at zero rpm.

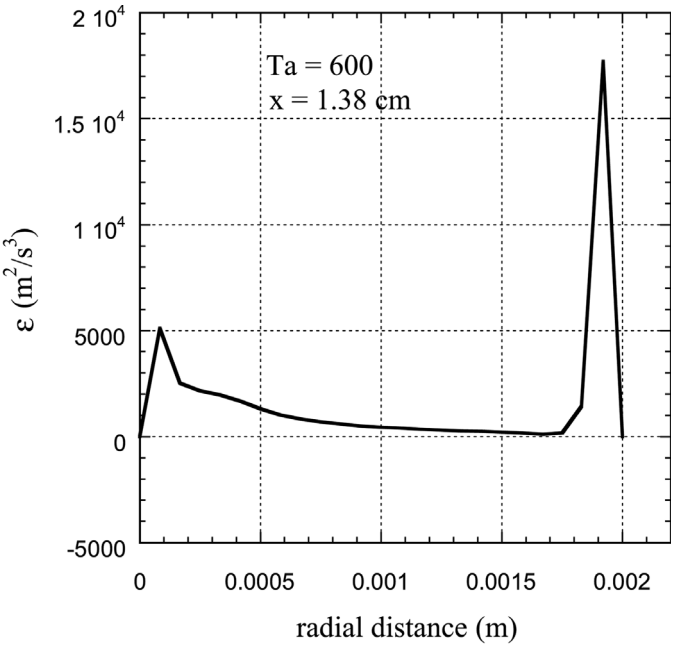

Figure 7. Eddy dissipation across gap.

Power Consumption

The energy input per unit volume ε_v of liquid flowing through the Taylor column for all of the data was computed from the expression for power/mass P_m where

$$P_m = \frac{C_m}{4}\left(\frac{U_i^3}{d}\right) \tag{4}$$

Thus, the energy per unit volume

$$\varepsilon_v = P_m \tau \bar{\rho} \tag{5}$$

where τ is the residence time (holdup volume/ total volume flowrate) and $\bar{\rho}$ is the average fluid density of the water–toluene mixture.

Since the torque coefficient C_m depends on the Taylor number Ta, values of Ta were determined from Eq. (1). Estimates were also made for the viscosity of

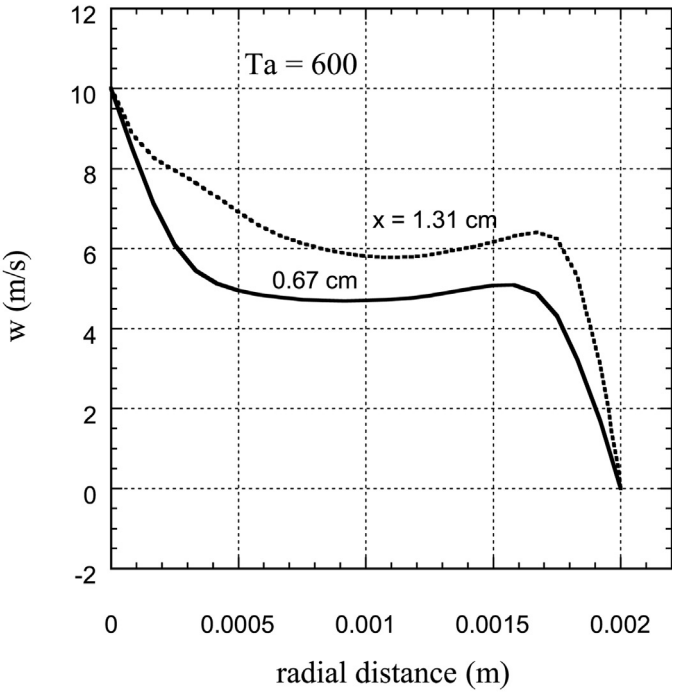

Figure 8. Velocity (peripheral) across gap.

the two-phase mixtures μ_m from the expression,[12]

$$\mu_m = \frac{\mu_c}{\phi_c}\left(1 + \frac{1.5\mu_d\phi_d}{\mu_d + \mu_c}\right) \tag{6}$$

where ϕ is the volume fraction of each fluid and the subscript c, d refer to the continuous and disperse phase, respectively.

For the data with equal volume flowrates of water and toluene or $\phi_c = \phi_d \cong 0.5$, either $\mu_m = 2.58\,\mu_w$ if water is assumed to be the disperse phase or $\mu_m = 1.81\,\mu_w$ for a disperse phase of toluene. Thus, the average of both values was assumed or $\mu_m = 2.2\,\mu_w$ for these data. Likewise, for the second set of runs with a volume flowrate ratio of 9.5:1 for water-to-toluene, the toluene was assumed to be dispersed or $\phi_c \cong 0.905$ for water while $\phi_d \cong 0.095$ for toluene giving $\mu_m = 1.2\,\mu_w$.

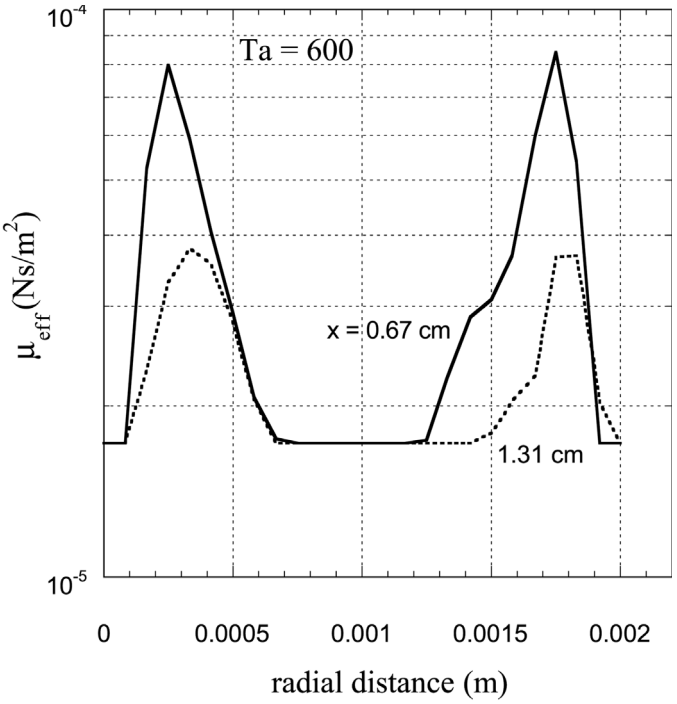

Figure 9. Effective viscosity.

Stage Efficiency

The data representing stage efficiency E_a due to agitation in the Taylor column [Eq. (3)] was plotted on the ordinate shown in Fig. 12 vs. energy per unit volume ε_v defined by Eq. (5). These data closely follow the pattern of the results of Flynn and Treybal[13] and Treybal.[14] In the latter case, either 6 or 12 in stirred tanks were used for turbulent fluid agitation where each tank contained four baffles and a six-bladed turbine impeller. These tanks represent a scale-up in the holdup volume of 10^3-10^4 compared to the present model Taylor column.

Values for the energy per unit volume ε_v from Eqs. (4) and (5) are plotted on the abscissa shown in Fig. 12. The ε_v values were determined from a graph of the torque coefficient C_m vs. Taylor number Ta provided in Schlichting.[9] Values of the Taylor number Ta for the mass flow ratio of 1.2 in Fig. 12 varied over the range $100 < Ta < 200$ for $E_a < 1$ and $Ta > 400$ for $E_a = 1$. The former corresponds to laminar vortex flow for a single phase. In contrast, all of the data for a water–toluene mass flow ratio of 11 covered a range $600 < Ta < 1000$ that

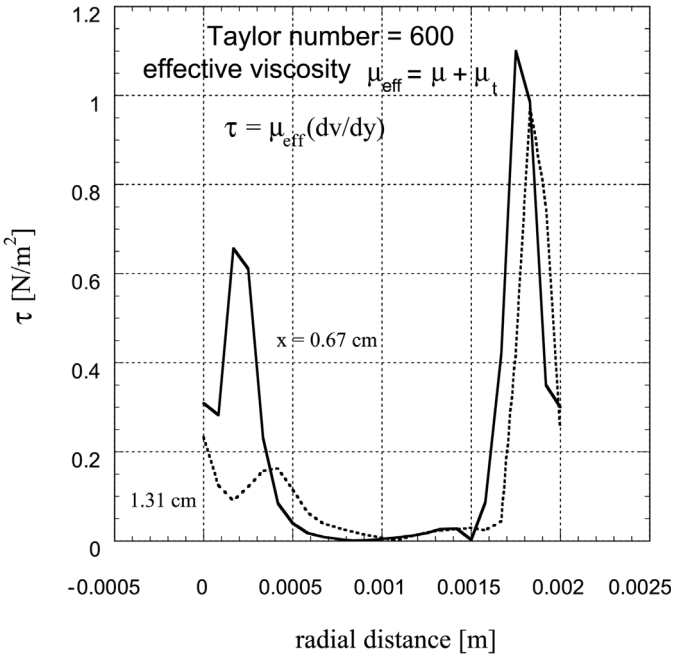

Figure 10. Shear stress across gap.

produces single-phase turbulent vortex flow. Of course, the character of the flow and the influence of the second phase on the transition value of $Ta = 400$ from laminar-to-turbulent flow is at present unknown.

We note from Fig. 12 that the stage efficiency E with agitation increases with an increase in the ratio of flowrates of disperse-to-continuous phase. It is of interest to consider the effect of the disperse phase volume fraction ϕ_d on the fractional extraction or stage efficiency E in our work. Assuming a continuous-phase controlled system throughout (in our case the aqueous phase when benzoic acid is the solute), it is unfortunate that no correlation exists for the continuous-phase mass transfer coefficient, k_c, around the swarm of drops present in a Taylor vortex column. But perhaps a tenuous analogy can be drawn with the case of a swarm of drops present in an agitated vessel for a two-phase liquid–liquid system for which a correlation does exist, fortunately in terms of ϕ_d.

From Skelland and Moeti[15] the correlation for k_c in agitated baffled vessels is

$$k_c = c_1 \phi_d^{-1/2} \tag{7}$$

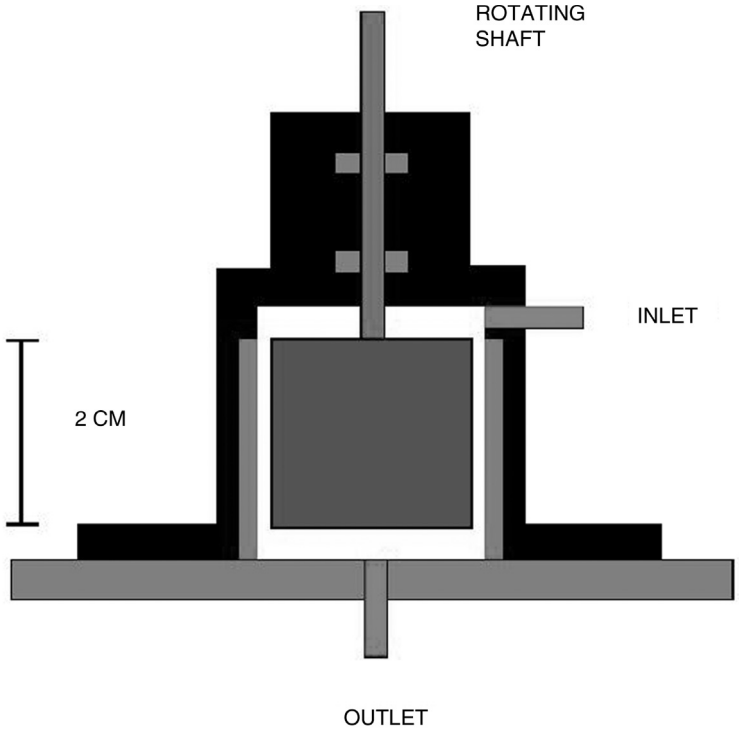

Figure 11. Schematic of Taylor vortex column; gap width = 2 mm, fluid volume = 6 mL.

where for a continuous-phase controlled system $k_c \cong K_c = mK_d$ and m is a constant distribution ratio (disperse phase concentration/continuous phase concentration of solute at equilibrium). If the total drop surface area is $A_d = c_2\phi_d$, a balance on solute transfer during time dt is

$$K_d A_d(c_B^* - c_B)dt = V_d dc_B \tag{8}$$

where $V_d = c_3\phi_d$ is the volume of disperse phase in the column at any instant, c_B the concentration of benzoic acid in the disperse phase, and c_B^* is the disperse phase concentration of benzoic acid that would be in equilibrium with that existing in the continuous phase. Substituting $K_d \cong k_c/m$, $V_d = c_3\phi_d$ and Eq. (7) into Eq. (8), one obtains

$$\alpha\phi_d^{-1/2}(c_B^* - c_B)dt = dc_B \tag{9}$$

where $\alpha = c_1c_2/mc_3$.

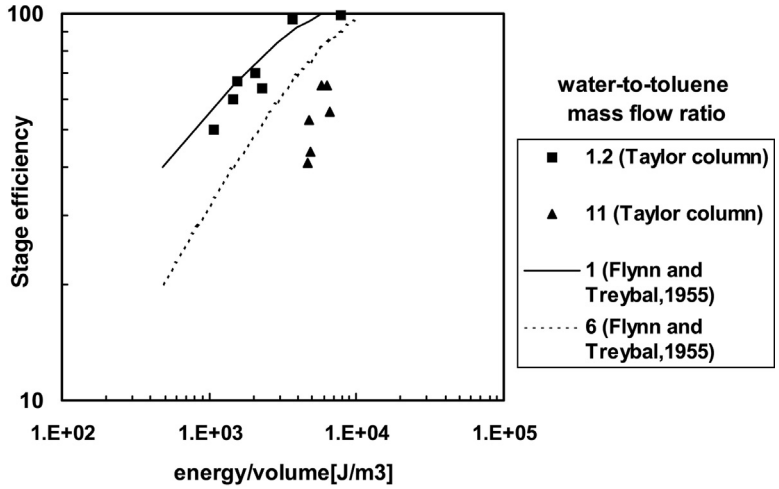

Figure 12. Comparison of the liquid–liquid extraction data for toluene–water–benzoic acid. Vertical axis is the single-stage efficiency due to rotation. Lines are large (several liters) stirred tank data from Flynn and Treybal.[13] Symbols are the present data in a small 6-mL Taylor column.

Regarding c_B^* as a constant at its average value and integrating Eq. (9) from CB1 (inlet) to CB2 (outlet) over the residence time t_r, one obtains

$$-\ln\left[\frac{c_B^* - c_{B2}}{c_B^* - c_{B1}}\right] = -\ln\left[\frac{c_B^* - c_{B1}}{c_B^* - c_{B1}} - \frac{c_{B2} - c_{B1}}{c_B^* - c_{B1}}\right] = -\ln[1 - E]$$

$$= \alpha\phi_d^{-1/2} t_r \tag{10}$$

The quantity t_r is the average residence time of the dispersed phase in the contacting volume V_S in the unit, or

$$t_r = \phi_d V_S / q_{dF} \tag{11}$$

where q_{dF} is the volumetric flowrate of the disperse phase through the volume V_S. From Eqs. (10) and (11), the stage efficiency now becomes

$$E = 1 - \exp[-\alpha(V_S/q_{dF})\phi_d^{1/2}] \tag{12}$$

where α is a constant for a given geometry, agitation rate, fluid system, and flowrate of the disperse phase q_{dF}.

Much data in the literature suggest that dispersion and mixing may be incomplete at lower agitation rates where for most cases of interest, that is, for a disperse phase less dense than the continuous phase, one observes $\phi_d < \phi_{dF}$ where $\phi_{dF} = (q_{dF}/q_{cF})/(1 + q_{dF}/q_{cF})$ based on feed flowrates. Skelland and Seksaria,[16] for example, recorded six distinct types of two-phase liquid–liquid dispersions at lower impeller speeds. The data of Weinstein and Treybal[17,18] indicate that ϕ_d/ϕ_{dF} is a constant for a given geometry, agitation rate, fluid system, and feed rate of the disperse phase, while being independent of the flowrate of the continuous phase. Regarding the last point, Flynn and Treybal[13] also state that "the degree of initial dispersion in the vessel is more a function of solvent than of water flow rate."

Thus, rewriting the exponent in Eq. (12) in the form

$$\alpha(V_S/q_{dF})(\phi_d/\phi_{dF})^{1/2}\phi_{dF}^{1/2} = \beta\phi_{dF}^{1/2} \tag{13}$$

where β is a constant for the restrictions just noted above for constant ϕ_d/ϕ_{dF}, the efficiency E becomes

$$E = 1 - \exp\left[-\beta\phi_{dF}^{1/2}\right] \tag{14}$$

Equation (14) supports the experimental data of Fig. 12 indicating an increase in the efficiency, E with increasing volume fraction of disperse phase based on feed conditions.

It is an interesting apparent difference between continuous and batch operation that has prompted these attempts to isolate the influence of the disperse phase holdup ϕ_d. They indicate that its positive effects on interfacial area, solute holding capacity, and disperse phase residence time outweigh its negative effect on the mass transfer coefficient.

However, for batch operation, in contrast, the residence time t_r in Eq. (10) becomes the run time and is thus no longer dependent on ϕ_d. In this case Eq. (10) now predicts the opposite effect of ϕ_d on E from that observed in Fig. 12. The latter finding is directionally consistent with the experimental findings of Miller and Mann[19] and Hixson and Smith[20] in batch-operated agitated vessels.

CONCLUSIONS

The Taylor vortex column is much easier to scale-up than conventional mixing devices such as stirred tanks and static mixers. The power consumption is attributable to friction rather than form drag, which makes the device particularly useful in shear-sensitive mixing applications. Moreover, unlike a stirred tank, one can scale-up to larger volumes while maintaining both constant power/volume and shear stress.

The CFD simulations of single phase flow in a Taylor column demonstrate that the presence of the Taylor vortices (secondary flow) has little effect on the mean flow velocity and pressure distribution. Turbulent flow properties such as turbulent dissipation rate and effective viscosity, however, are strongly affected by the secondary flow. In particular, there is a large peak in the turbulent dissipation rate at the stagnation points along both the rotor and the stator walls. The effect, however, of the dispersed phase on the flow characteristics are not known at present.

The extraction, single-stage efficiency in a small model Taylor column was demonstrated to conform to the pattern of data previously measured by Flynn and Treybal[13] in a much larger (and more complex) stirred tank. These results would suggest that mass transfer rates in liquid–liquid extraction processes are not particularly sensitive to the details of power input per unit volume but that similar results can be obtained with radically different and simpler flow patterns. The simple design of a concentric rotating flow in a Taylor column, for example, will provide equivalent results.

APPENDIX

If the stage efficiency due to agitation is defined as

$$E_a = (E - E_o)/(1 - E_o) \tag{A1}$$

and the stage efficiency is defined as

$$E = 1 - \exp[-\alpha(V_S/Q)(\phi_{dF})^m] \tag{A2}$$

where $\alpha = \alpha(P/Q$, fluid properties, tank geometry, feed rate of dispersed phase).

Then the stage efficiency with no agitation must be of the form

$$E_o = 1 - \exp[-\alpha_o(V_S/Q)(\phi_{dF})^n]. \tag{A3}$$

Thus one obtains

$$E_a = 1 - \exp[-\{\alpha(\phi_{dF})^m - \alpha_o(\phi_{dF})^n\}(V_S/Q)]. \tag{A4}$$

Since the data for E_a is independent of the residence time V_S/Q, the following must hold

$$[\alpha(\phi_{dF})^m - \alpha_o(\phi_{dF})^n] = (Q/V_S)f(\phi_{dF}, P/Q) \tag{A5}$$

for fixed tank geometry, fluid properties, and feed rate of dispersed phase.

Equation (5) states that at small residence times the effects of agitation are large for both equal power input per unit flowrate and volume fraction of dispersed phase.

ACKNOWLEDGMENTS

The authors gratefully acknowledge the contributions from Dow Corning Corp., Fluent Inc., and Holl Technologies Inc.

REFERENCES

1. Uhl, V.W.; Von Essen, J.A. In *Mixing: Theory and Practice*; Uhl, V.W.; Gray, J.B.; Eds.; Academic Press: London, 1986; Vol. 3, Chap. 15, 216–220.
2. Oldshue, J.Y. *Fluid Mixing Technology*; McGraw-Hill: New York, 1983.
3. Baier, G.; Grateful, T.M.; Graham, M.D.; Lightfoot, E.N. Prediction of Mass Transfer Rates in Spatially Periodic Flows. Chem. Eng. Sci. **1999**, *54*, 343–355.
4. Davies, M.W.; Weber, E.J. Liquid–Liquid Extraction Between Rotating Concentric Cylinders. Ind. Eng. Chem. **1960**, *52*, 929–934.
5. Forney, L.J.; Morris, J.; Skelland, A.H.P.; Holl, R. Taylor Vortex Column: Large Shear for Two-Phase Flows, Paper 162a, Annual AIChE Meeting, Dallas, Texas, 1999.
6. Leonard, R.A.; Berstein, G.J.; Pelto, R.H.; Ziegler, A.A. Liquid–Liquid Dispersion in Turbulent Couette Flow. AIChE J. **1981**, *27*, 495–503.
7. Baier, G.; Graham, M.D.; Lightfoot, E.N. Mass Transfer in a Novel Two-Fluid Taylor Vortex Extractor. AIChE J. **2000**, *46*, 2395–2407.
8. Baier, G.; Graham, M.D. Two-Fluid Flow: Experiments and Linear Theory for Immiscible Liquids Between Corotating Cylinders. Phys. Fluid **1998**, *10*, 3045–3055.
9. Schlichting, H. *Boundary Layer Theory*, 7th Ed.; McGraw-Hill: New York, 1979.
10. Schmidt, W.; Kossak, S.; Langenbuch, J.; Hermann, C.; Kremeskotter, H. 6th International Workshop on Polymer Reaction Engineering, Berlin, 1998.
11. Moore, C.; Cooney, C. Axial Dispersion in a Taylor–Couette Flow. AIChE J. **1995**, *41*, 723–727.
12. Skelland, A.H.P. Interphase Mass Transfer. In *Science and Practice of Liquid–Liquid Extraction*; Thornton, J.D., Ed.; Clarendon Press: Oxford, 1992; Chap. 2, 278–279.
13. Flynn, A.W.; Treybal, R.E. Liquid–Liquid Extraction in Continuous-Flow Agitated Extractors. AIChE J. **1955**, *1*, 324–328.
14. Treybal, R.E. *Liquid Extraction*, 2nd Ed.; McGraw-Hill: New York, 1963.

15. Skelland, A.H.P.; Moeti, L.T. Mechanism of Continuous-Phase Mass-Transfer in Agitated Liquid Liquid-Systems. Ind. Eng. Chem. Res. **1990**, *29*, 2258–2267.
16. Skelland, A.H.P.; Seksaria, R. Minimum Impeller Speeds for Liquid–Liquid Dispersion in Baffled Vessels. I&EC Process Des. Dev. **1978**, *17*, 56–61.
17. Weinstein, B.; Treybal, R.E. Dispersed Phase Holdup in Baffled Vessels. AIChE J. **1973**, *19*, 851–852.
18. Weinstein, B.; Treybal, R.E. Liquid–Liquid Contacting in Unbaffled, Agitated Vessels. AIChE J. **1973**, *19*, 304–312.
19. Miller, S.A.; Mann, C.A. The Theory of Short-Circuiting in Continuous Flow Mixing Vessels. Trans. Am. Inst. Chem. Eng. **1934**, *31*, 409–456.
20. Hixson, A.W.; Smith, M.I. Mass Transfer in Liquid–Liquid Agitation Systems. Ind. Eng. Chem. **1949**, *41*, 973–978.

Received September 2001
Revised March 2002